Functional entry of members of Venezuelan Equine Encephalitis Complex into host cells is dependent on clathrin-mediated endocytosis, in a pH-dependent manner

Lucia Maria Ghietto[1, †], Pedro Ignacio Gil[1, †], Paloma Olmos Quinteros[1], Emiliano Gomez[1], Franco Martin Piris[1], Patricia Kunda[1, 3], Marta Contigiani[1], Maria Gabriela Paglini[1, 2, *].

[1]Instituto de Virología "Dr. JM Vanella", Facultad de Ciencias Médicas, Universidad Nacional de Córdoba, Córdoba, Argentina.

[2]Instituto de Investigación Médica Mercedes y Martín Ferreyra, INIMEC-CONICET-Universidad Nacional de Córdoba, Córdoba, Argentina.

[3]Centro de Investigación en Medicina Traslacional "Severo Amuchástegui" (CIMETSA), Instituto Universitario Ciencias Biomédicas Córdoba (IUCBC), Naciones Unidas 420, Córdoba, Argentina

[†]**These authors have contributed equally to this work**

*** Corresponding author:**
María Gabriela Paglini, Ph.D.
Instituto de Virología "Dr. JM Vanella"
Facultad de Ciencias Médicas,
Universidad Nacional de Córdoba, Córdoba, Argentina.
Phone: +54-351-4681465 (ext. 105) Fax: +54-351-4695163.
E-mail: gpaglini@immf.uncor.edu

Abstract

Pixuna virus (PIXV) and Río Negro virus (RNV) are mosquito-borne alphaviruses belonging to the Venezuelan Equine Encephalitis (VEE) complex, which includes pathogenic epizootic and enzootic subtypes responsible for life-threatening diseases in equines. Considering that the first steps in viral infection are crucial for the efficient production of new progeny, the aim of this study was to elucidate early events of the replication cycle of these two viruses. To this end, we used chemical inhibitors and the expression of dominant-negative constructs to study the dependence of clathrin and endosomal pH on PIXV and RNV internalization mechanism. We demonstrated that both viruses are internalized primarily via clathrin-mediated endocytosis, where the low pH of endosomes is crucial for viral replication. Contributing knowledge the entry route of VEE complex members is important to understand the pathogenesis of these viruses and to develop new antiviral strategies.

Keywords: Pixuna virus, Rio Negro virus, Alphavirus, entry, endosomes

1. Introduction

Venezuelan equine encephalitis (VEE) antigenic complex belongs to the Togaviridae family, Alphavirus genus, it constitutes a group of arboviruses responsible for outbreaks of human and veterinary disease around the world, [1] sharing similar genetic characteristics and can be defined by broad antigenic cross-reactivity [2]. The VEE complex comprises New World viruses that cause encephalitis in humans and horses and are classified in six antigenic subtypes divided into epizootic (IAB and IC) and enzootic subtypes [3]. One of the members of VEE complex is Pixuna virus (PIXV), New World alphavirus subtype IV [4]. PIXV was first isolated from Anopheles nimbus mosquitoes in Brazil in 1961 [5]. It has been detected in Argentina [6,7] and it is a non pathogenic member of the complex. Another member is Rio Negro virus (RNV), subtype VI, that circulates in Argentina [6,8] and has been isolated from rodents [9]. In 1989, RNV caused an outbreak of acute febrile illness in humans, which was originally attributed to dengue virus due to the similarity of the symptoms [9]. Enzootic subtypes, including PIXV and RNV, are also important to human health because they can cause febrile illnesses with similar clinical symptoms to those caused by dengue or influenza (headache, chills, fever, myalgia, retroocular pain) [10].

Viruses use the host cell machinery for entry, replication, transport and release of the viral progeny; and the first steps in viral infection are crucial for the efficient production of new progeny. The different stages of replication cycle of the enzootic variants of the VEE complex are still poorly studied. Even though, studies on alphaviruses have demonstrated that, after binding to receptors on the plasma membrane, enter into the cell via clathrin-mediated endocytosis and fusion with endosomal membranes [11-13]. However, the mechanisms concerning the cell biology of alphaviruses infection are unclear since some authors described other pathways for cell penetration, including caveolae-dependent endocytosis [14], the direct delivery through a putative pore at the plasma membrane [15] or macropinocytosis-mediated

uptake [16]. In this sense, and considering that the entry route of different enzootic variants of the VEE complex remain poorly explored, it is important to describe the mechanisms of entry and uncoating of these viruses. Therefore, the aim of the present research was to elucidate the early events of the replication cycle of two enzootic members of the VEE complex: PIXV and RNV. To this end, we used chemical inhibitors and the expression of dominant-negative constructs to study the dependence of clathrin and endosomal pH on PIXV and RNV internalization mechanism. We demonstrate that both viruses are internalized primarily via clathrin-mediated endocytosis, where the low pH of endosomes is crucial for viral replication. The results reported here show new insights regarding the entry and infection of VEE complex members. In addition, these findings provide a better understanding of the molecular mechanisms underlying their replication cycle pointing to attractive targets for the development of strategies to prevent infections.

2. Results

2.1. Clathrin is required for PIXV and RNV to entry into Vero cells

Considering that the ability of alphaviruses to enter to the host cell via alternative pathways has already been reported [17], we evaluated the dependence of PIXV and RNV entry into Vero cells by clathrin-mediated endocytosis. To this end, we first employed chemical inhibitors of clathrin-mediated endocytosis, such as sucrose (SCR) and chlorpromazine (CPZ). According to the literature and to the possible drug-induced cytotoxic effects, cell culture viability by MTT was assayed at different concentrations of these inhibitors (Figure 1A). Thus, we defined 0.2 M for SCR and 25 uM for CPZ as the experimental conditions. Besides, the inhibitory action of both drugs on clathrin-mediated endocytosis was effectively assessed determining the diminution of TRITC-transferrin internalization. The fluorescence inside the

cell cytoplasm observed in cultures treated with SCR or CPZ was significantly lower (64.6% and 55.9%, respectively; $p < 0.001$) compared to control cells (100%, Figure 1B). After PIXV or RNV internalization, in the presence of drugs, we collected the supernatants at 4, 8 and 24 hours postinfection (hpi) and quantified extracellular infectious particles by plaque assay (plaque-forming unit, PFU/ml). Infected cultures with PIXV (multiplicity of infection: MOI 0.1) and treated with 0.2 M SCR or 25 uM CPZ showed a significant decrease in PUF/ml of about 2 $\log_{10}$ and 1-2 $\log_{10}$ at 8 and 24 hpi, respectively. In the same way, infected cultures with RNV (MOI 0.1) and treated with both drugs displayed a significant reduction of virus particles in the extracellular medium of about 1-2 $\log_{10}$ and 2 $\log_{10}$ at 8 and 24 hpi, respectively (Figure 1C). Additionally, cell cultures were treated and infected with PIXV or RNV (MOI 10). At 8 hpi, cultures were fixed and processed for immunofluorescence in order to calculate the percentage of infected cells. In the representative image, the culture shows a visible reduction of green fluorescence labeling of culture after treatment with both inhibitors in comparison to mock-treated cells (Figure 1D). Cultures treated with SCR or CPZ showed a significant reduction in the percentage of PIXV (67.83 ± 3.68 and 56.15± 25.85, respectively; $p < 0.001$) and RNV (51.17 ±18.49 and 21.49 ± 16.7 respectively; $p < 0.001$) infected cells with respect to control (100%). Additionally, we observed significant differences between both drugs in cultures infected with RNV (Figure 1E).

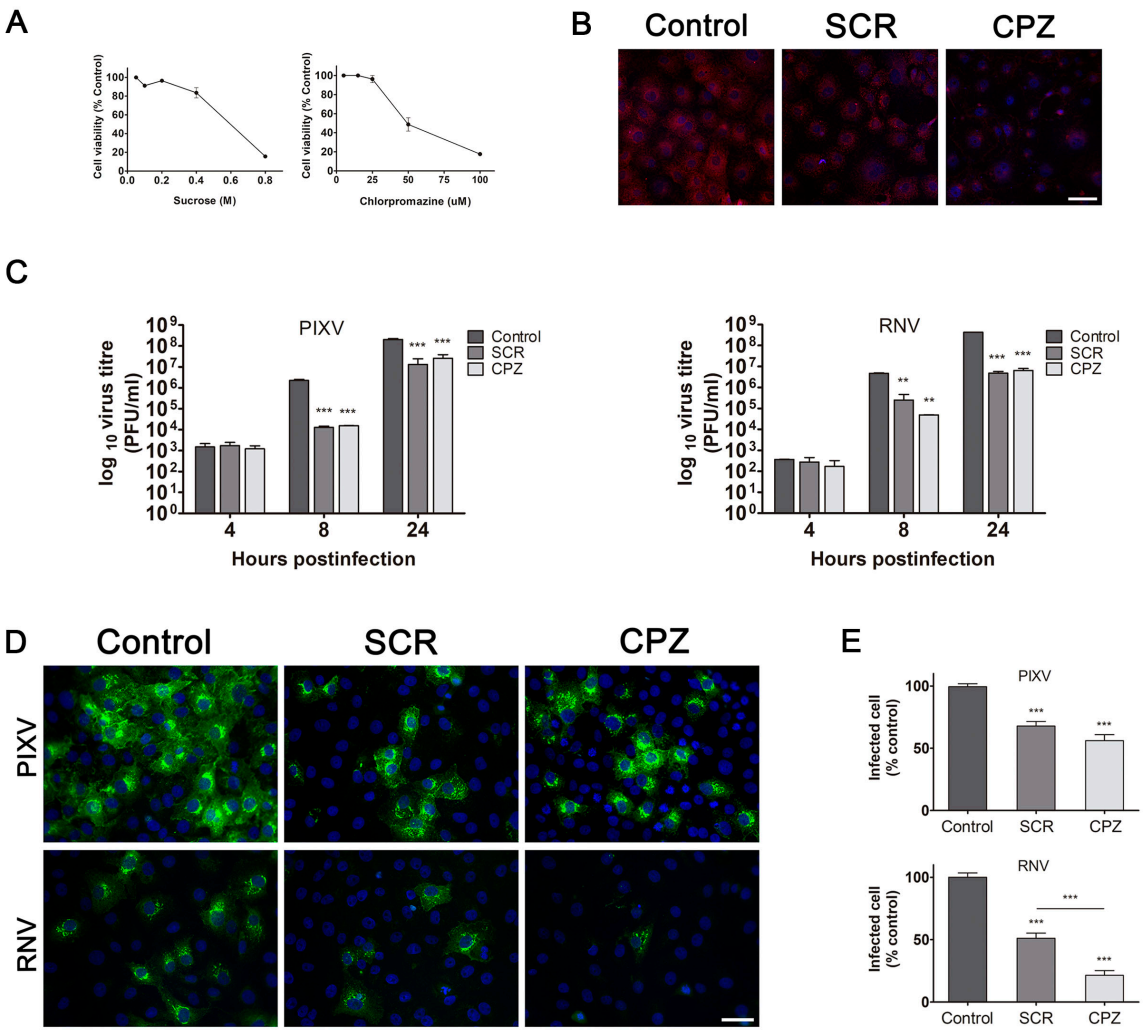

Figure 1. Assays with inhibitors targeting clathrin-mediated endocytosis of PIXV and RNV entry. A. MTT assay to determine cytotoxic concentration of SCR and CPZ. **B.** Representative images of Vero cells treated with 0.2 M SCR or 25 uM CPZ and incubated with TRITC-transferrin (transferrin in red and nuclei in blue). **C.** Cells were treated with 0.2 M SCR or 25 uM CPZ and infected with PIXV or RNV at MOI 0.1. Supernatants were collected at 4, 8 and 24 hpi and extracellular infectious particles were quantified by plaque assay (plaque-forming unit, PFU/ml). **D**. Representative images of cultures treated with 0.2 M SCR or 25 uM CPZ and infected with PIXV (green) or RNV (green); nuclei (blue) at MOI 10 and fixed at 8 hpi. **E**. Percentage of infected cells, infected with PIXV or RNV was calculated quantifying more than 300 cells per condition from three independent experiments. Data

represent the mean ± SD of 3 independent experiments. Significance was calculated by one-way ANOVA test, followed by Tukey post-hoc analysis to enable specific group comparison, with p value ≤ 0.05 considered as statistically significant. **$p < 0.01$; ***$p < 0.001$. Scale bar: 20 µm.

To support the participation of the clathrin pathway in PIXV and RNV entry, we employed wild type (WT) and dominant negative (DN) mutant constructs of the clathrin-coat associated cellular protein Eps15, a required adaptor for clathrin-mediated endocytosis [18]. Vero cells were transfected with plasmids expressing Eps15-WT or Eps15-DN; and their functionality was confirmed by incubation of transfected cells with TRITC-transferrin. Eps15-DN expression remarkably reduced transferrin internalization (Figure 2A) in comparison to cultured cells expressing Eps15-WT. Transiently transfected cells with either Eps15-WT or Eps15-DN were then infected with PIXV or RNV (MOI 10) and the effect of the expression of mutant proteins on the internalization of both viruses was analyzed at 8 hpi by immunofluorescence (Figure 2B). No significant difference was found in the percentage of infection in all cultures transfected under both conditions (24.51 ± 10.53 Eps15-WT; 19.18 ± 7.75 Eps15-DN for PIXV and 14.74 % ± 2.38 Eps15-WT; 12.34 ± 5.35 Eps15-DN for RNV). Quantification of the transfected/infected cells showed a significant reduction ($p < 0.001$) of about 60% of infection in Eps15-DN condition relative to Eps15-WT for both viruses (Figure 2C). Taken together, these results provide strong evidence that clathrin plays an important role for both PIXV and RNV entry.

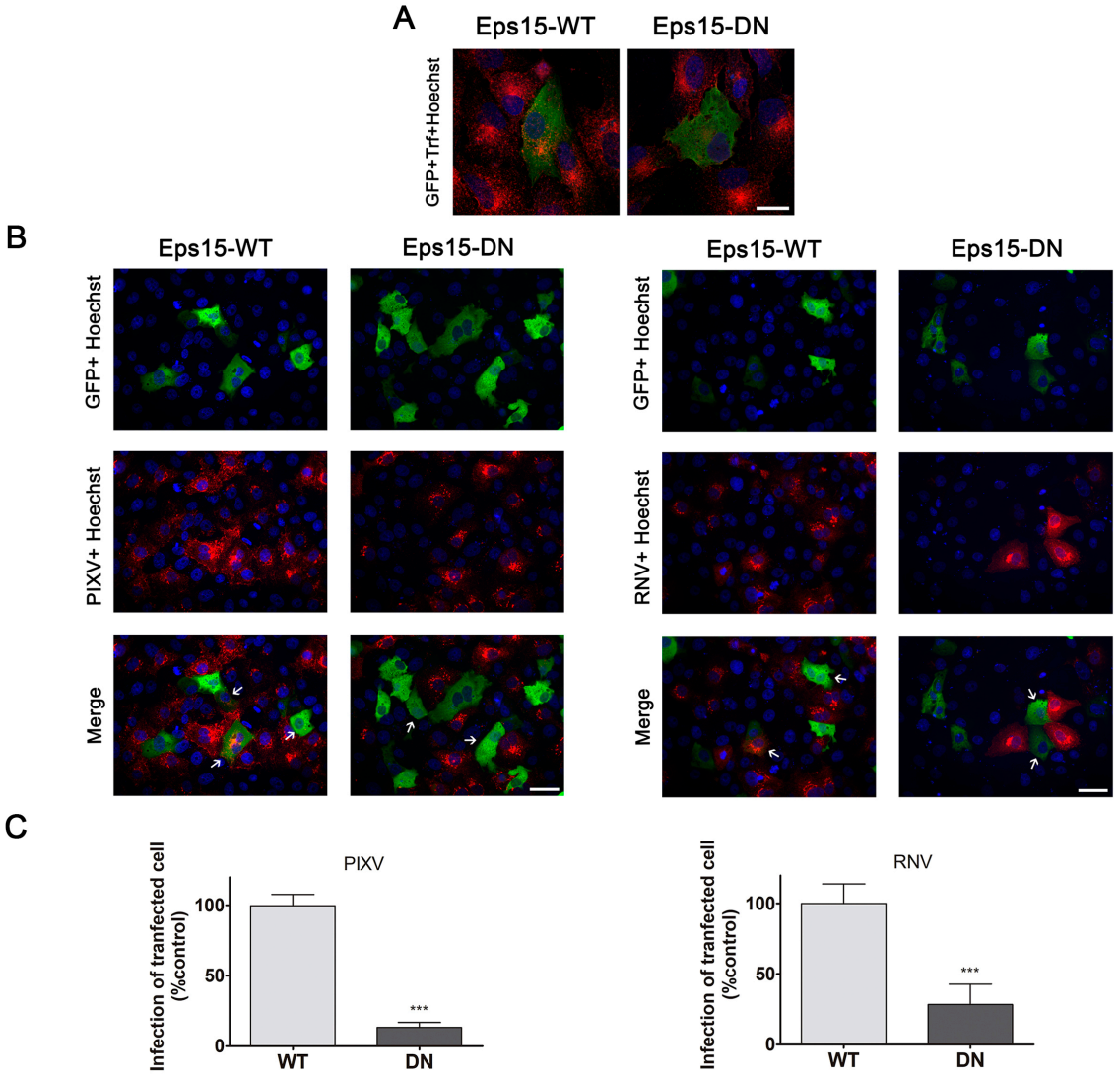

Figure 2. Inhibition of PIXV and RNV entry by transient expression of Eps15 dominant negative mutant construct. A. Representative images of cells transfected with plasmids expressing Eps15-WT (green) or Eps15-DN (green) and incubated with TRITC-transferrin (red). **B.** Immunofluorescence of transiently transfected cells with plasmids expressing Eps15-WT or Eps15-DN and infected with PIXV or RNV (arrow) at MOI 10 after 8 hpi (red). **C.** Percentages of transfected and infected cells. More than 300 transfected cells were screened in each case. Data represent the mean ± SD from 3 independent experiments. Significance was calculated by Student's t test, with p value ≤ 0.05 considered as statistically significant. ***p < 0.001. Scale bar: 20 µm.

2.2 PIXV and RNV infection requires active endosomal acidification

Endosomal vesicles may play a crucial role in virus infection, providing the appropriate condition for conformational changes in envelope viral proteins, resulting in the formation of a fusion pore and release of the viral nucleocapsid into the cytosol [19]. Considering that the endocytic pathway is highly regulated and involves several intermediate organelles, it is important to examine the fate of viral proteins after their internalization in early and late endosomes. The Rab family of small GTPases is essential for membrane trafficking and the classification of endocytic loads into specific subcellular compartments [20]. In this sense, we performed a quantitative colocalization analysis of PIXV and RNV with Rab5-GFP and Rab7-GFP, as early and late endosome markers, respectively [21] (Figure 3A). Using Pearson's colocalization coefficient [22], we observed significant colocalization PIXV and RNV proteins with Rab5-GFP and Rab7-GFP (Figure 3A). After 8 hpi, a great coefficient of colocalization was found for both endosomal compartments and the viral proteins (PIXV: $r= 0.68 \pm 0.11$ for Rab5 and $r= 0.78 \pm 0.06$ for Rab7; RNV: $r=0.69 \pm 0.1$ for Rab5 and $r= 0.75\pm 0.07$ for Rab7) (Figure 3B). These results show that PIXV and RNV require trafficking to early and late endosomes to initiate an infectious cycle.

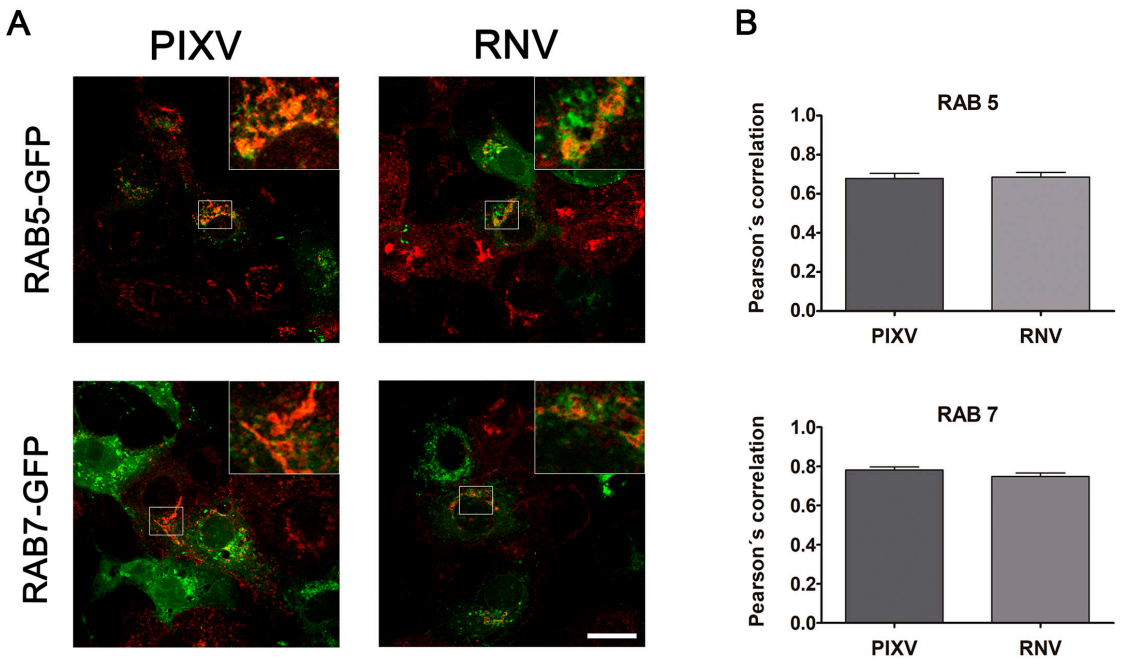

Figure 3: Colocalization of PIXV and RNV with Rab5 and Rab7. **A.** Immunofluorescence of transiently transfected cells with plasmids expressing Rab5-GFP or Rab7-GFP and infected with PIXV or RNV at MOI 10 (red). **B.** Colocalization analyses for Rab5-GFP or Rab7-GFP expression with PIXV or RNV were expressed as Pearson's correlation coefficient. The plots show the mean of Pearson's correlation coefficients ± SD from three independent experiments. Scale bar: 20 µm.

To study the low pH-dependence of PIXV and RNV replication, we first evaluated the effect of two lysosomotropic agents, Glucosamine (GlcN) and ammonium chloride (NH_4Cl), inhibitors of endosomal vesicles acidification, in Vero cells. Cell culture viability by MTT was assayed at different concentration of either of these two inhibitors. The cytotoxicity test showed that 50 mM GlcN and 25 mM NH_4Cl do not affect cell viability (Figure 4A). Therefore, these concentrations were defined as the experimental conditions. To assure the effect of both compounds in intracellular acidic vesicles, we pretreated Vero cells with the

drugs plus acridine orange. As we expected, acridine orange did not accumulate in endosomal vesicles in cultures treated with GlcN, however, this effect was not observed in culture cells treated with NH_4Cl (Figure 4B). Therefore, we then performed the cytoplasmic accumulation assay with neutral red, a very sensitive probe for lysosomal microenvironments and a biological pH indicator [23]. In figure 3C it can be seen an inhibition of neutral red signal of 40% and 80% in cultures treated with GlcN and NH_4Cl, respectively, compared to untreated cells. The participation of endosomal pH in PIXV and RNV replication in Vero cells was analyzed by extracellular virus titration. Viral progeny production of PIXV and RNV was reduced by about 3 $\log_{10}$ and 4 $\log_{10}$ in cultures incubated with GlcN or NH_4Cl respectively, at 8 and 24 hpi, compared to control cultures (Figure 4D). The fluorescence pattern of intracellular PIXV proteins observed in control cultures was substantially reduced in cells treated with GlcN or NH_4Cl. In cultures infected with RNV, fluorescence was completely lost when cells were treated with both compounds (Figure 4E). A reduction of 50% was detected in the number of cells expressing PIXV proteins in cultures treated with GlcN and approximately 100% in NH_4Cl compared to untreated infected ones. Interestingly, the percentage of RNV infected cells was practically zero in cultures treated with both lysosomotropic agents (Figure 4F).

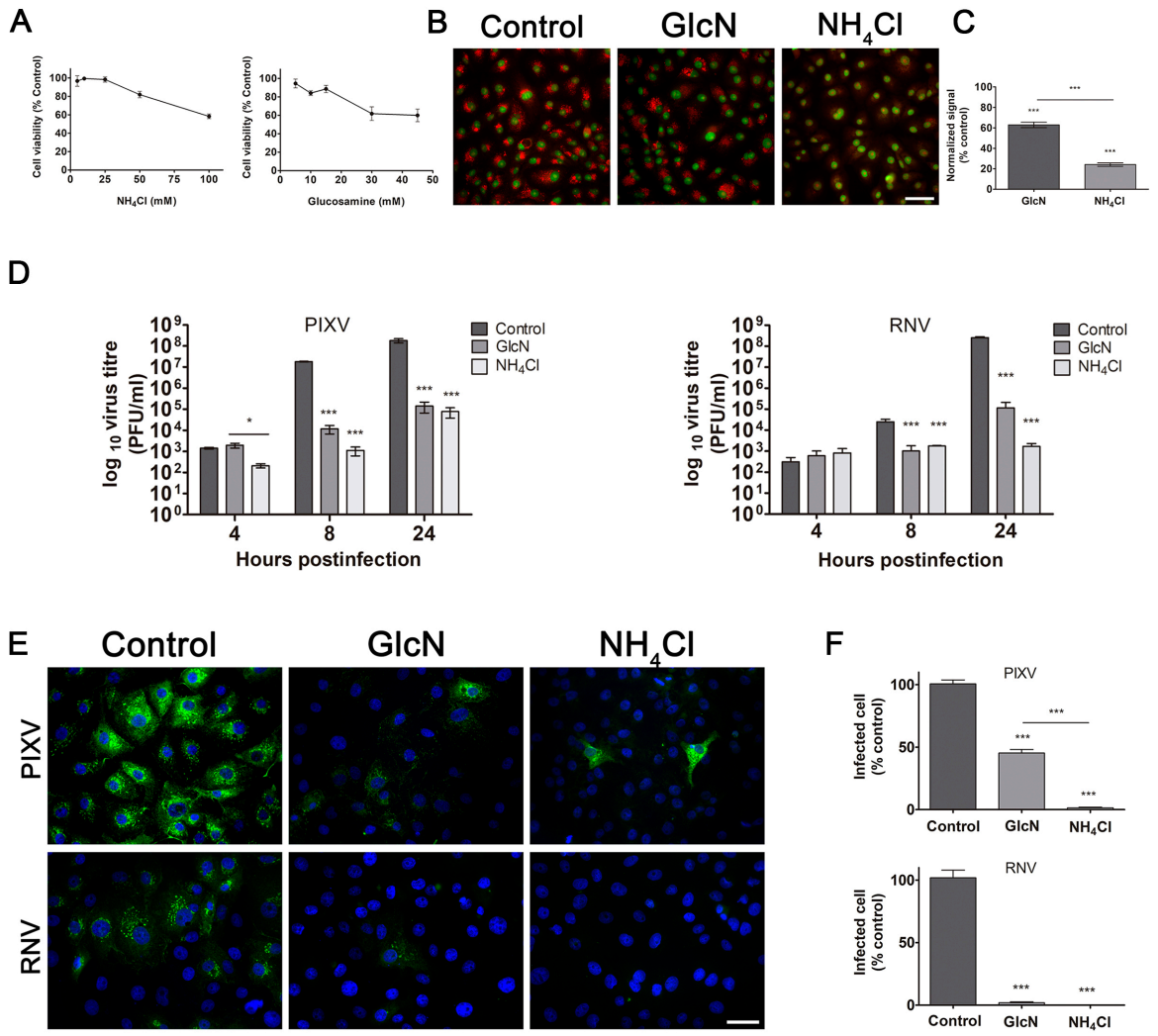

Figure 4. Effect of lysosomotropic agents on PIXV and RNV internalization. A. MTT assay to determine cytotoxic concentration of GlcN and NH_4Cl. **B.** Representative images of Vero cells treated with 50 mM GlcN or 25 mM NH_4Cl and incubated with acridine orange (red) **C.** Vero cells incubated with 50 mM GlcN or 25 mM NH_4Cl and neutral red (NR). Percentages of inhibition were calculated by absorbance compared to control cultures. **D.** Cells were pretreated with 50 mM GlcN or 25 mM NH_4Cl and infected with PIXV or RNV at MOI 0.1 (Green). Supernatants were collected at 4, 8 and 24 hpi and extracellular infectious particles were quantified by plaque assay (plaque-forming unit, PFU/ml). **E**. Representative images of cultures treated with 50 mM GlcN or 25 mM NH_4Cl and infected with PIXV (green) or RNV (green); nuclei (blue) at MOI 10 and fixed at 8 hpi. **F**. Percentage of infected

cells with PIXV or RNV was calculated quantifying more than 300 cells per condition from three independent experiments. Data represent the mean ± SD of 3 independent experiments. Significance was calculated by one-way ANOVA test, followed by Tukey post-hoc analysis to enable specific group comparison, with p value ≤ 0.05 considered as statistically significant. *$p < 0.05$; **$p < 0.01$; ***$p < 0.001$. Scale bar: 20 μm.

3. Discussion

Alphaviruses constitute a conserved group of arboviruses responsible for outbreaks of human and veterinary disease around the world [1]. The VEE complex comprises varieties of enzootic and epizootic viruses. The epizootic strains emerge periodically in regions of Central America and northern areas of South America, causing outbreaks that involve humans and horses, with high morbidity and mortality rates [1,2]. In particular, Venezuelan Equine Encephalitis virus (VEEV) is the most important zoonotic pathogen, with several reported outbreaks in South and Central America [24]. Alphaviruses are enveloped viruses that generally penetrate into the cells by different ways: by fusion with the cell plasma membrane or by receptor-mediated endocytosis; a pathway that usually relies on the low pH of the endocytic vesicles. Different endocytic pathways have been characterized over the past decade, among which the clathrin-mediated endocytosis is one of the most commonly used entry route by many enveloped viruses [25]. Moreover, this is the most widely accepted mechanism for alphaviruses entry and the subsequent fusion between the viral envelope and the endosomal membrane [26]. However, some reports showed alternative pathways, such as early endosomes and caveolae-derived vesicles for Mayaro virus in Vero cells [14], the direct delivery through a putative pore at the plasma membrane for Sindbis virus [15], or macropinocytosis for Chikungunya virus (CHIKV) entry into human muscle cells [16]. To investigate whether two members of the VEE antigenic

complex, use clathrin in the endocytic pathway in Vero cells, various systematic approaches were used. These include pharmacological inhibition and overexpression of Eps15 WT and DN mutant plasmids. Our results suggest that infection of target cells depends, in part, on clathrin-mediated endocytosis as endocytic inhibitors only resulted in partial block of PIXV and RNV infection. This supports the hypothesis that several pathways are used by alphaviruses to facilitate their entry into target cells [27]. It is well known that actin assembly plays an essential role in several processes leading to endocytosis, including the internalization of clathrin-coated vesicles [28]. In agreement with previous literature, our work supports the notion that PIXV and RNV use clathrin-mediated endocytosis as the major/principal pathway to enter into the host cell. In this sense, previous results from our laboratory demonstrated that PIXV relies on a dynamic actin network during the early steps of viral replication. This indicates that specific interactions with cytoskeletal proteins are necessary for the normal development of viral replication [29]. Different members of the alphavirus genus have been reported to enter host cells using this pathway [27]. Nevertheless, mutants of Eps15 and Rab5, as well as endocytic inhibitors only resulted in partial block in CHIKV infection, supporting the hypothesis that several pathways are hijacked by the virus to facilitate its entry into target cells [30,31]. In line with this idea, Lee and collaborators demonstrate that entry of CHIKV into human muscle cells is mediated by macropinocytosis [16]. Besides, new findings show that VEEV and Western equine encephalitis virus exploit the caveolin-1-mediated transcytosis via to enter the central nervous system [32], providing alternative pathways for virus entry in different types of cells. For example, as described for Influenza virus, clathrin-endocytosis and macropinocytosis can operate simultaneously in HeLa, A549 and other non-human cells [33]. Considering that PIXV and RNV entry depends only in part on clathrin-mediated endocytosis, it would be interesting to study alternative pathways that might be used to facilitate their entry into target cells.

In alphaviruses, as well as in other viruses, the progressive pH decrease in the maturing endocytic pathway triggers events in the viral envelope proteins resulting in viral uncoating. The E2 envelope protein mediates viral entry by attachment to cellular receptors. Then, the low-pH environment triggers a sequence of events starting with the dissociation of the E1-E2 dimer and followed by conformational changes in the E1 membrane fusion protein. This sequence of events results in the formation of a fusion pore and the release of the viral ARN into the cytosol [27,34]. Almost all viruses that are internalized by the cell via endocytosis are first delivered to Rab5-positive early endosomes before being targeted to Rab5/Rab7-positive maturing endosomes, Rab7-positive late endosomes, and lysosomes [35]. Our results show that PIXV and RNV proteins colocalize with both, early and late endosomes, suggesting that these viruses enter the endocytic pathway of the host cell and require trafficking as far as early and late endosomes to initiate an infectious cycle. Previous studies on alphaviruses revealed that Semliki Forest virus fused with early endosomes, and VEEV was found to fuse with maturing and/or late endosomes [11-13]. In CHIKV, membrane fusion was observed predominantly with Rab5-positive endosomes and often occurred within 40 s after delivery to endosomes [31]. To further confirm our observations, we employed lysosomotropic agents to interfere with endosome acidification, extensively used as an assay for alphaviruses entry [11,36]. As expected, PIXV and RNV required a progressive pH reduction in endosomes in order to release the viral nucleic acid into the cytosol.

In conclusion, this study demonstrates, for the first time, that PIXV and RNV partially enter via clathrin-dependent endocytosis into Vero cells. Then, both viruses require transport to early and late endosomes, where the acidic pH-dependent step results in the release of PIXV or RNV RNA into the cytoplasm for a successful infection. This study contributes to our understanding of the entry process in enzootic subtypes of the VEE complex. Considering that arthropod borne viruses are significant sources of disease in man and domestic animals, this

research extends the knowledge of virus entry into host cells and provide a better understanding of the molecular mechanisms underlying the viral internalization process. Ultimately, this knowledge will be useful to develop potent antivirals that could block the virus at the early stages of infection.

4. Materials and Methods

4.1. Cell culture and viruses

Vero cells (Vero 76, ATCC CRL 1587) were grown in Dulbecco's modified Eagle's medium (DMEM) (GIBCO, USA) with 10% fetal calf serum (FCS), Gentamicin (50 µg/ml), at 37 °C, 5% CO2 and 98% humidity. The PIXV strain BeAr 35645, isolated from *Anopheles nimbuspor* in Brazil (Shoper et al., 1964), it was propagated in Vero cells and stocks were stored at 2×10^8 plaque-forming units (PFU/ml). The RNV strain AG80-663 was isolated from *Culex delpontei* in 1980 [37], it was propagated in Vero cells and stocks were stored at 7×10^8 PFU/ml. Virus inoculum (PFU/ml) was determined by a standard plaque assay.

4.2. Virus titration

Infected Vero cell monolayers were overlaid with 1.5% ultra-pure agarose (Gibco BRL) n 4% DMEM 2x. Two days later, the cells were fixed with 10% formaldehyde in water and the overlaid medium was removed. The monolayers were stained with 1% crystal violet in water and the plaques were counted. Infectivity titers were expressed as PFU/ml. All the experiments with viruses were performed in a laminar flow hood under biosafety level 2 conditions.

4.3. Drug treatments

Chlorpromazine (CPZ) was used in this study as an inhibitor of clathrin-mediated endocytosis [38]. Sucrose (SCR) was used to generate a hypertonic medium to disturb the formation of clathrin vesicles on the cell membrane [39]. Glucosamine (GlcN) and ammonium chloride (NH_4Cl) were used to elevate the pH of acidic organelles. All drugs were dissolved in phosphate-buffered saline (PBS) to prepare master-stocks for storage [40-42]. All compounds were purchased from Sigma-Aldrich. Vero cell monolayers were seeded into 6-well plates or 24-well plates and pretreated with drugs, as listed before, for 30 min at 4 °C. Adsorption and internalization of PIXV and RNV was achieved by infecting the cells at MOI of 0.1 and 10 at 4 °C for 1 h in the presence of the compounds. Then, the inoculum was removed and MEM was added with different inhibitors throughout all designed experiments. In cultures infected at MOI 0.1, the supernatant was collected at 4, 8 and 24 hpi to determine extracellular viruses by a titration assay. Monolayers infected with MOI 10 were fixed at 8 hpi to proceed to an immunofluorescence assay to determine intracellular viruses. To evaluate the efficiency of blockade of each endocytic pathway by the different inhibitors, uptake studies with TRITC-transferrin to SCR and CPZ, neutral red and acridine orange to NH_4Cl and GlcN were performed. Untreated cells were used as control. Cells either treated with inhibitors or not, were incubated with 15 μg/ml TRITC-transferrin and 100 μg/ml acridine orange (A6014, Sigma) in serum free medium during 15 min at 37°C. Then, cells were processed for visualization in a fluorescence microscope as described below. To determine inhibition by lysosomotropic agents, we incubated cultured cells with drugs at a selected concentration plus 50 mg/ml neutral red (NR), as a biological lysosomal pH indicator. Cells were seeded in 100 μl per well of transparent 96-well microtiter plates. Following drug treatments, the cell culture medium was replaced with medium containing 50 μg/ml NR dye and drugs. Following incubation for 3 ± 0.5 h at 37 °C and 5% CO2 in a humidified environment and two washes with PBS, intracellular NR dye was extracted using a destaining solution (50% ethanol, 1%

acetic acid and water) and absorbance was measured at 540 nm using a spectrophotometer (Biotek, Elx800). Percentage of inhibition of each drug was calculated normalizing data against the negative control absorbance (considered as the 100% value).

4.4. Viability assay

Cell viability drug treatments were assessed by employing 3-(4 5-dimethylthiazol-2-yl)-5-(3-carboxymethoxyphenyl)-2-(4-sulfophenyl)-2h-tetrazolium (MTT). Briefly, Vero cells were seeded at the density of 1×10^6 cells/well in a 96-well plate. After 24 h, cells were treated with drugs at different concentrations for 24 h, untreated cells served as control. After treatment, cells were washed with PBS and 100 µl MTT assay was mixed with 900 µl PBS into each well, followed by incubation at 37 °C for 2 h. The medium was then removed, washed, and 1 ml DMSO was added to each well. After gentle mixing, the absorbance was measured using an ELISA plate reader at 570 nm wavelength. Only DMSO was used as the blank (medium) control. The concentration (for each drug) that caused only a 20% reduction in metabolic activity was used in subsequent experiments.

4.5. Cell transient transfection

The plasmids for EPS15 wild-type WT (Eps15-WT) and dominant negative DN Δ95/295 (Eps15-DN) constructs, both containing proteins fused to GFP, were kindly provided by Dra. Nathalie Sauvonnet (Institut Pasteur, Paris, France). The GFP tagged constructs of Rab5 and Rab7 were provided by Jose Luis Daniotti and Alejandro Vilcaes (CIQUIBIC-FCQ-UNC-CONICET). Vero cells grown to 70% confluence were transiently transfected using polyethylenimine (PEI). In brief, 2 ug of plasmid were mixed in 125 ul of ClNa 150 mM and 3 ul of PEI in MEM. After 24 h of culture, fluorescence was observed under an epifluorescence microscope (Olympus IX81 epifluorescence inverted microscope). Transfected cell cultures were infected with PIXV or RNV at MOI 10. The percentage of

infection was calculated by scoring the number of cells positive for the viral antigen in approximately 300 transfected cells with comparable levels of GFP expression (15 microscopy fields). For colocalization coefficients, images were taken whit a Confocal Zeiss LSM 800 microscope. For the analysis, images were first deconvoluted using the PSF Generator and Deconvolution lab plug-in (Biomedical Imaging group) of the FIJI software [43]. The PSF for each image was obtained applying the Born and Wolf optical model to the images using PSF Generator plug-in of the FIJI software. Then, images were deconvoluted applying the FIJI software Richardson and Lucy algorithm in Deconvolution lab plug-in. After that, for each cell, a focal plane was selected for analysis using a Pearson's correlation coefficient. The resulting coefficient value was the average of selected image areas containing predominantly colocalization in 10 cells from 3 independent cell cultures.

4.6. Viral infection

The protocol of synchronized infection has been previously described by Gil and col (Gil et al., 2017). Vero cells were plated and incubated at 37 °C, 5% CO2 and 98% humidity. Confluent monolayers of Vero cells were infected at different multiplicity of infection (MOI) 0.1 for standard plaque assays and MOI 10 and for immunofluorescence assays. Virus adsorption was performed at 4 °C per 1 h. After this first incubation, the inoculum was removed and monolayers were washed with PBS at 4 °C to eliminate any free virus particle and DMEM with 1% FCS was added before incubating at 37 °C, 5% CO2 and 98% humidity for 8, 12 or 24 h, depending on the experiment. The cytopathic effect was evaluated by direct visualization by phase contrast microscopy at low magnification using an Olympus IX81 microscope.

4.7. Inmunofluorescence assay

We performed a previously described assay [29]. Briefly, cell monolayers were grown at 70% confluence on glass coverslips, washed three times with PBS, fixed with 4% paraformaldehyde/1% sucrose (Riedel-de Haën, Sigma-Aldrich Laborchemikalien GmbH, Seelze, Germany) for 20 min at room temperature (RT) and then washed with PBS. The cells were then permeabilized with 0.2% TritonTM X-100 (Sigma-Aldrich, St. Louis, MO) in PBS for 5 min at RT and incubated with 5% bovine serum albumin (BSA, Sigma-Aldrich, St. Louis, MO) for 1h at RT. In order to detect viral structural proteins, cells were incubated with an anti-PIXV-RNV primary polyclonal IgG antibody generated in mice in our laboratory, diluted 1/1000 in 1% BSA/PBS solution over night at 4 °C. Then, monolayers were washed three times with PBS, and incubated with the secondary antibodies (goat anti-mouse Alexa Fluor 488 and Alexa Fluor 647, Thermo Fisher Scientific Inc., Waltham, Massachusetts, USA) for 2h at RT. To visualize the actin filaments, the fixed and permeabilized cell monolayers were labeled with Phalloidin-Tetramethyl rhodamine B (Sigma-Aldrich, St. Louis, MO) for 1h at RT. Cells were visualized using a conventional inverted epifluorescence microscope (Olympus IX81, Olympus Corporation, Shinjuku, Tokyo). Images were processed off line using Adobe Photoshop CS6 (Version: 13.0). Percentage of infected cells was calculated quantifying more than 300 cells per condition in each independent experiment.

4.8. Statistical analysis

All tests and graphs were performed using GraphPad Prism 5. Data are representative of at least three independent experiments and values are given as mean ± standard deviation (SD). Statistical analyses were carried out using unpaired student *t*-test and one-way ANOVA test, followed by a Tukey post-hoc analysis to enable specific group comparison (Type I error set at 0.05), as appropriate.

5. References

1 Griffin, D. E. *Fields' Virology* (eds David M. Knipe & Peter M. Howley) Ch. 23, 651 (Wolters Kluwer/Lippincott Williams & Wilkins Health, 2013).

2 Weaver, S. C., Winegar, R., Manger, I. D. & Forrester, N. L. Alphaviruses: population genetics and determinants of emergence. *Antiviral Res.* **94**, 242-257, doi:S0166-3542(12)00085-X [pii];10.1016/j.antiviral.2012.04.002 [doi] (2012).

3 Forrester, N. L. *et al.* Evolution and spread of Venezuelan equine encephalitis complex alphavirus in the Americas. *PLoS neglected tropical diseases* **11**, e0005693, doi:10.1371/journal.pntd.0005693 (2017).

4 Weaver, S. C. Arrival of chikungunya virus in the new world: prospects for spread and impact on public health. *PLoS neglected tropical diseases* **8**, e2921, doi:10.1371/journal.pntd.0002921 (2014).

5 Shoper, R. E., Causey, O. R. & de Aandrade, A. H. The venezuelan equine encephalomyelitis complex of group a arthropod-borne viruses, including mucambo and pixuna from the amazon region of brazil. *Am.J Trop.Med.Hyg.* **13**, 723-727 (1964).

6 Albrieu-Llinas, G. *et al.* Arbovirus serosurvey (Orthobunyavirus, Flavivirus, and Alphavirus) in a draft horse population from Santa Fe, Argentina (2013-2016). *Archives of virology* **166**, 881-884, doi:10.1007/s00705-020-04929-4 (2021).

7 Pisano, M. B. *et al.* Cocirculation of Rio Negro Virus (RNV) and Pixuna Virus (PIXV) in Tucuman province, Argentina. *Trop.Med.Int.Health* **15**, 865-868 (2010).

8 Pisano, M. B. *et al.* First detection of Rio Negro virus (Venezuelan equine encephalitis complex subtype VI) in Cordoba, Argentina. *Mem Inst Oswaldo Cruz* **107**, 125-128 (2012).

9 Contigiani, M. S. *et al.* [Presence of antibodies against Venezuelan equine encephalitis virus subtype VI in patients with acute febrile illness]. *Rev Argent Microbiol* **25**, 212-220 (1993).

10 Aguilar, P. V. *et al.* Endemic Venezuelan equine encephalitis in the Americas: hidden under the dengue umbrella. *Future Virol* **6**, 721-740, doi:10.2217/FVL.11.5 (2011).

11 Colpitts, T. M., Moore, A. C., Kolokoltsov, A. A. & Davey, R. A. Venezuelan equine encephalitis virus infection of mosquito cells requires acidification as well as mosquito homologs of the endocytic proteins Rab5 and Rab7. *Virology* **369**, 78-91, doi:S0042-6822(07)00477-1 [pii];10.1016/j.virol.2007.07.012 [doi] (2007).

12 Kolokoltsov, A. A., Fleming, E. H. & Davey, R. A. Venezuelan equine encephalitis virus entry mechanism requires late endosome formation and resists cell membrane cholesterol depletion. *Virology* **347**, 333-342 (2006).

13 Leung, J. Y., Ng, M. M. & Chu, J. J. Replication of alphaviruses: a review on the entry process of alphaviruses into cells. *Adv Virol* **2011**, 249640, doi:10.1155/2011/249640 (2011).

14 Carvalho, C. A. M., Silva, J. L., Oliveira, A. C. & Gomes, A. M. O. On the entry of an emerging arbovirus into host cells: Mayaro virus takes the highway to the cytoplasm through fusion with early endosomes and caveolae-derived vesicles. *PeerJ* **5**, e3245, doi:10.7717/peerj.3245 (2017).

15 Vancini, R., Wang, G., Ferreira, D., Hernandez, R. & Brown, D. T. Alphavirus genome delivery occurs directly at the plasma membrane in a time- and temperature-dependent process. *J Virol.* **87**, 4352-4359, doi:JVI.03412-12 [pii];10.1128/JVI.03412-12 [doi] (2013).

16 Lee, C. H. R., Mohamed Hussain, K. & Chu, J. J. H. Macropinocytosis dependent entry of Chikungunya virus into human muscle cells. *PLoS neglected tropical diseases* **13**, e0007610, doi:10.1371/journal.pntd.0007610 (2019).

17 Kononchik, J. P., Jr., Hernandez, R. & Brown, D. T. An alternative pathway for alphavirus entry. *Virol.J* **8**, 304, doi:1743-422X-8-304 [pii];10.1186/1743-422X-8-304 [doi] (2011).

18 Mettlen, M., Chen, P. H., Srinivasan, S., Danuser, G. & Schmid, S. L. Regulation of Clathrin-Mediated Endocytosis. *Annu Rev Biochem* **87**, 871-896, doi:10.1146/annurev-biochem-062917-012644 (2018).

19 White, J. M. & Whittaker, G. R. Fusion of Enveloped Viruses in Endosomes. *Traffic* **17**, 593-614, doi:10.1111/tra.12389 (2016).

20 Homma, Y., Hiragi, S. & Fukuda, M. Rab family of small GTPases: an updated view on their regulation and functions. *The FEBS journal* **288**, 36-55, doi:10.1111/febs.15453 (2021).

21 Stenmark, H. Rab GTPases as coordinators of vesicle traffic. *Nature reviews. Molecular cell biology* **10**, 513-525, doi:10.1038/nrm2728 (2009).

22 Adler, J. & Parmryd, I. Quantifying colocalization by correlation: the Pearson correlation coefficient is superior to the Mander's overlap coefficient. *Cytometry. Part A : the journal of the International Society for Analytical Cytology* **77**, 733-742, doi:10.1002/cyto.a.20896 (2010).

23 Sousa, C. *et al.* Solvent polarity and pH effects on the spectroscopic properties of neutral red: application to lysosomal microenvironment probing in living cells. *Photochemistry and photobiology* **63**, 601-607, doi:10.1111/j.1751-1097.1996.tb05662.x (1996).

24 Taylor, K. G. & Paessler, S. Pathogenesis of Venezuelan equine encephalitis. *Vet Microbiol* **167**, 145-150, doi:10.1016/j.vetmic.2013.07.012 (2013).

25 Sieczkarski, S. B. & Whittaker, G. R. Dissecting virus entry via endocytosis. *Journal of General Virology* **83**, 1535-1545 (2002).

26 Vancini, R., Hernandez, R. & Brown, D. Alphavirus entry into host cells. *Prog Mol Biol Transl Sci* **129**, 33-62, doi:10.1016/bs.pmbts.2014.10.002 (2015).

27 Holmes, A. C., Basore, K., Fremont, D. H. & Diamond, M. S. A molecular understanding of alphavirus entry. *PLoS pathogens* **16**, e1008876, doi:10.1371/journal.ppat.1008876 (2020).

28 Mooren, O. L., Galletta, B. J. & Cooper, J. A. Roles for actin assembly in endocytosis. *Annu.Rev.Biochem.* **81**, 661-686, doi:10.1146/annurev-biochem-060910-094416 [doi] (2012).

29 Gil, P. I. *et al.* Pixuna virus modifies host cell cytoskeleton to secure infection. Manuscrito en Revisión. Scientific Reports. (2017).

30 Bernard, E. *et al.* Endocytosis of chikungunya virus into mammalian cells: role of clathrin and early endosomal compartments. *PloS one* **5**, e11479 (2010).

31 Hoornweg, T. E. *et al.* Dynamics of Chikungunya Virus Cell Entry Unraveled by Single-Virus Tracking in Living Cells. *Journal of virology* **90**, 4745-4756, doi:10.1128/JVI.03184-15 (2016).

32 Salimi, H. *et al.* Encephalitic Alphaviruses Exploit Caveola-Mediated Transcytosis at the Blood-Brain Barrier for Central Nervous System Entry. *mBio* **11**, doi:10.1128/mBio.02731-19 (2020).

33 de Vries, E. *et al.* Dissection of the influenza A virus endocytic routes reveals macropinocytosis as an alternative entry pathway. *PLoS pathogens* **7**, e1001329, doi:10.1371/journal.ppat.1001329 (2011).

34 Vaney, M. C., Duquerroy, S. & Rey, F. A. Alphavirus structure: activation for entry at the target cell surface. *Curr.Opin.Virol.* **3**, 151-158, doi:S1879-6257(13)00041-2 [pii];10.1016/j.coviro.2013.04.003 [doi] (2013).

35 Yamauchi, Y. & Helenius, A. Virus entry at a glance. *Journal of cell science* **126**, 1289-1295, doi:10.1242/jcs.119685 (2013).

36 Schuchman, R. M. *et al.* Role of the vacuolar ATPase in the Alphavirus replication cycle. *Heliyon* **4**, e00701, doi:10.1016/j.heliyon.2018.e00701 (2018).

37 Mitchell, C. J. *et al.* Arbovirus investigations in Argentina, 1977-1980. II. Arthropod collections and virus isolations from Argentine mosquitoes. *The American journal of tropical medicine and hygiene* **34**, 945-955 (1985).

38 Sieczkarski, S. B. & Whittaker, G. R. Influenza Virus Can Enter and Infect Cells in the Absence of Clathrin-Mediated Endocytosis. *Journal of virology* **76**, 10455-10464 (2002).

39 Chen, C. L. *et al.* Inhibitors of clathrin-dependent endocytosis enhance TGFbeta signaling and responses. *Journal of cell science* **122**, 1863-1871, doi:10.1242/jcs.038729 (2009).

40 Dean, R. T., Jessup, W. & Roberts, C. R. Effects of exogenous amines on mammalian cells, with particular reference to membrane flow. *Biochem J* **217**, 27-40 (1984).

41 Garda, H. & Paglini, S. Efecto de la D-glucosamina sobre la replicación del virus pixuna en cultivo de células de embrión de pollo. *Revista latinoamericana de microbiologia* **25**, 221-223 (1983).

42 Lin, Y. *et al.* Glucosamine promotes hepatitis B virus replication through its dual effects in suppressing autophagic degradation and inhibiting MTORC1 signaling. *Autophagy* **16**, 548-561, doi:10.1080/15548627.2019.1632104 (2020).

43 Sage, D. *et al.* DeconvolutionLab2: An open-source software for deconvolution microscopy. *Methods* **115**, 28-41, doi:10.1016/j.ymeth.2016.12.015 (2017).

6. Acknowledgements

We would like to thank Laura Fozzatti, Javier Aguilar, Brenda Konigheim, Guillermo Albrieu-Llinás and Pablo Lopez for generously providing some reagents; Gonzalo Quasollo and Cecilia Sampedro for technical assistance in confocal microscopy at the Centro de Micro y Nanoscopía de Córdoba, CEMINCO-CONICET-Universidad Nacional de Córdoba, Córdoba, Argentina. We particularly thank to Srta. Stella Ascheri for general technical assistance. This work was supported by grants from Secretaria de Ciencia y Tecnología - Universidad Nacional de Córdoba (SECYT-Consolidar-C Nº 33620180100091CB), Ministerio de Ciencia, Tecnología e Innovación, Gobierno de Córdoba (GRFT 77/19), and Agencia Nacional de Promoción Científica y Tecnológica Argentina (FONCYT PICT/18-02423).

7. Author contribution

All authors were responsible for the design of the study. LMG, PIG, POQ and EG performed the experimental procedures and collected data. LMG, PIG and FMP conducted statistical data analysis. LMG, PIG and PK performed imaging analysis. PK, MC and MGP contributed ideas and comments. LMG, PIG, MC and MGP interpreted the findings and drafted the manuscript. Supervision and project administration were done by MGP and funding's acquisition by MGP, LMG and PIG. All authors critically reviewed the contents and approved the final version for publication.

8. Additional Information

Competing Interests: The authors declare no conflict of interest

9. Figure Legends

Figure 1. Assays with inhibitors targeting clathrin-mediated endocytosis of PIXV and RNV entry. A. MTT assay to determine cytotoxic concentration of SCR and CPZ. **B.** Representative images of Vero cells treated with 0.2 M SCR or 25 uM CPZ and incubated with TRITC-transferrin (transferrin in red and nuclei in blue). **C.** Cells were treated with 0.2 M SCR or 25 uM CPZ and infected with PIXV or RNV at MOI 0.1. Supernatants were collected at 4, 8 and 24 hpi and extracellular infectious particles were quantified by plaque assay (plaque-forming unit, PFU/ml). **D**. Representative images of cultures treated with 0.2 M SCR or 25 uM CPZ and infected with PIXV (green) or RNV (green); nuclei (blue) at MOI 10 and fixed at 8 hpi. **E**. Percentage of infected cells, infected with PIXV or RNV was calculated quantifying more than 300 cells per condition from three independent experiments. Data represent the mean ± SD of 3 independent experiments. Significance was calculated by one-way ANOVA test, followed by Tukey post-hoc analysis to enable specific group comparison, with p value ≤ 0.05 considered as statistically significant. **$p < 0.01$; ***$p < 0.001$. Scale bar: 20 µm.

Figure 2. Inhibition of PIXV and RNV entry by transient expression of Eps15 dominant negative mutant construct. A. Representative images of cells transfected with plasmids expressing Eps15-WT (green) or Eps15-DN (green) and incubated with TRITC-transferrin (red). **B.** Immunofluorescence of transiently transfected cells with plasmids expressing Eps15-WT or Eps15-DN and infected with PIXV or RNV (arrow) at MOI 10 after 8 hpi (red). **C.** Percentages of transfected and infected cells. More than 300 transfected cells were screened in each case. Data represent the mean ± SD from 3 independent experiments. Significance was

calculated by Student's t test, with p value ≤ 0.05 considered as statistically significant. ***p < 0.001. Scale bar: 20 µm.

Figure 3: Colocalization of PIXV and RNV with Rab5 and Rab7. **A.** Immunofluorescence of transiently transfected cells with plasmids expressing Rab5-GFP or Rab7-GFP and infected with PIXV or RNV at MOI 10 (red). **B.** Colocalization analyses for Rab5-GFP or Rab7-GFP expression with PIXV or RNV were expressed as Pearson's correlation coefficient. The plots show the mean of Pearson's correlation coefficients ± SD from three independent experiments. Scale bar: 20 µm.

Figure 4. Effect of lysosomotropic agents on PIXV and RNV internalization. A. MTT assay to determine cytotoxic concentration of GlcN and NH_4Cl. **B.** Representative images of Vero cells treated with 50 mM GlcN or 25 mM NH_4Cl and incubated with acridine orange (red) **C.** Vero cells incubated with 50 mM GlcN or 25 mM NH_4Cl and neutral red (NR). Percentages of inhibition were calculated by absorbance compared to control cultures. **D.** Cells were pretreated with 50 mM GlcN or 25 mM NH_4Cl and infected with PIXV or RNV at MOI 0.1 (Green). Supernatants were collected at 4, 8 and 24 hpi and extracellular infectious particles were quantified by plaque assay (plaque-forming unit, PFU/ml). **E**. Representative images of cultures treated with 50 mM GlcN or 25 mM NH_4Cl and infected with PIXV (green) or RNV (green); nuclei (blue) at MOI 10 and fixed at 8 hpi. **F**. Percentage of infected cells with PIXV or RNV was calculated quantifying more than 300 cells per condition from three independent experiments. Data represent the mean ± SD of 3 independent experiments. Significance was calculated by one-way ANOVA test, followed by Tukey post-hoc analysis to enable specific group comparison, with p value ≤ 0.05 considered as statistically significant. *p < 0.05; **p < 0.01; ***p < 0.001. Scale bar: 20 µm.